Original article DOI: 10.2478/aiht-2023-74-3684

A new strategy to achieve high antimicrobial activity: green synthesised silver nanoparticle formulations with *Galium aparine* and *Helichrysum arenarium*

Cilem Ozdemir[1,2], Merve Gencer[1], Irem Coksu[3], Tulin Ozbek[1], and Serap Derman[3]

[1] Yıldız Technical University Faculty of Arts and Sciences, Department of Molecular Biology and Genetics, Istanbul, Turkey
[2] Mugla Sıtkı Kocman University Faculty of Medicine, Department of Medical Biology, Mugla, Turkey
[3] Yıldız Technical University Faculty of Chemical and Metallurgical Engineering, Department of Bioengineering, Istanbul, Turkey

[Received in October 2022; Similarity Check in October 2022; Accepted in June 2023]

Silver nanoparticles (AgNPs), which have recently gained attention due to their antimicrobial activity, can also be produced by green synthesis. The aims of this study were to (i) characterise green synthesized AgNPs using microwave-assisted aqueous extracts of *Galium aparine* (G-AgNPs) and *Helichrysum arenarium* (H-AgNPs) and (ii) investigate the combined antimicrobial effects of the G- and H-AgNPs in different ratios. Nanoparticle formation and reactions were determined with UV-Vis spectroscopy. The G-AgNPs were 52.0±10.9 nm in size, with a 0.285±0.034 polydispersity index (PDI), and a -17.9±0.9 mV zeta potential. For H-AgNPs these characteristics were 23.9±1.0 nm, 0.280±0.032, and -21.3±2.7 mV, respectively. Atomic force microscopy (AFM) and scanning electron microscopy (SEM) confirmed that the particles were monodisperse and spherical. The Fourier transform-infrared spectroscopy (FT-IR) results showed the presence of reducing agents that stabilised the AgNPs. Three different nanoformulations (NF-1, NF-2, and NF-3) were prepared by combining these two synthesised nanoparticles in different ratios and their antimicrobial activity was tested against *E. coli, S. aureus, C. albicans,* and *A. flavus*. Our study is the first to show that combining AgNPs from two different biological sources can produce effective nanoformulations with improved antibacterial activity against *E. coli* and *S. aureus*. These nanoformulations showed lower minimum inhibitory concentrations (31.25 μg/mL against *E. coli* with all NFs; 62.5 μg/mL for NF-1 and 125 μg/mL for NF-2/3 against *S. aureus*) than G-AgNPs (62.5 μg/mL for *E. coli*) or H-AgNPs (125 μg/mL for *S. aureus*) alone. Their high combined inhibitory effect against *E. coli* (NF-1–3) was synergistic and against *S. aureus* (NF-2 and NF-3) potentially additive. Considering such promising results, we believe our study provides some direction for new research and strategies in antimicrobial therapeutics.

KEY WORDS: *A. flavus*; antimicrobial nanosystems; *C. albicans*; *E. coli*; plant extracts; *S. aureus*; synergistic effect

Swift and remarkable advances in nanotechnology have made nanomaterials available for many applications in pharmacology, including transport and targeting of drug molecules, development of diagnostic imaging systems, design and production of controlled release systems, and support of plant nutrition (1–5). Nanoparticles can penetrate cells at a high rate thanks to their high surface area/volume ratio (6), and these properties provide nanoparticles with different biological activities such as antioxidant (7), antimicrobial (8, 9), and anticancer (10). Metallic nanoparticle systems have attracted particular attention in recent years, as, unlike polymeric or lipid nanoparticles, they can be used in antimicrobial treatment, especially due to their surface plasmon resonances (11–14). In this respect silver nanoparticles (AgNPs) stand out (15, 16).

Since chemical nanoparticle synthesis may involve many toxic agents, and physical synthesis is costly (17, 18), more and more attention is being given to the so called green nanoparticle synthesis, which relies on plants, microorganisms, algae, and DNA templates to reduce and stabilise nanoparticle metal ions (19–23). This is particularly true for AgNPs synthesised using plant extracts because of their broad antimicrobial spectrum (24, 25).

In this study, we wanted to see how extracts of immortelle (*Helichrysum arenarium*) and cleavers (clivers, bedstraw, *Galium aparine*) would fare in the synthesis of AgNPs in terms of their antimicrobial efficiency, considering that both plants have known therapeutic antimicrobial, antioxidant, and anticancer effects (26–37). In addition, both plants contain compounds that reduce silver and maintain the stability of the formed nanoparticles.

In this respect, high-efficiency extraction of plant components is the most crucial step in the green synthesis of AgNPs, and microwave-assisted extraction (MAE), which has earned it popularity in recent years, is more efficient and quicker than traditional extraction methods. In addition, MAE is a suitable for large-scale and small-scale systems (38).

Corresponding author: Serap Derman, Yıldız Technical University Faculty of Chemical and Metallurgical Engineering, Department of Bioengineering, 34210 Istanbul, Turkey, E-mail: *serapacar5@gmail.com*

To sum up, the aims of our study were to: (i) to synthesise and characterise two different AgNPs using the microwave-assisted aqueous extracts of *G. aparine* and *H. arenarium* (G-AgNP and H-AgNP, respectively) and (ii) to investigate the antimicrobial activity of combined nanoparticles at different ratios. To the best of our knowledge, this combination has not been investigated.

MATERIALS AND METHODS

Materials

Silver nitrate was purchased from Sigma-Aldrich (St. Louis, MO, USA). Müller Hinton broth, Müller Hinton agar, Sabouraud dextrose broth, and Sabouraud dextrose agar were purchased from Merck (Darmstadt, Germany). The plants *H. arenarium* and *G. aparine* were purchased commercially in dry form (Arpas Arifoglu Marketing Distribution and Trade Inc.). *E. coli* (ATCC number: 25922), *S. aureus* (ATCC number: 25923), *C. albicans* (ATCC number: 10231), and *A. flavus* (ATCC number: 204304) were obtained from the Yıldız Technical University Molecular Biology and Genetics Department, Laboratory of Microbiology (Istanbul, Turkey). Ultra-pure water was obtained from the Millipore MilliQ Gradient system (Millipore Corporation, Bedford, MA, USA).

Preparation of plant extracts

We opted for a fast, efficient, and environmentally friendly MAE method using water, a non-toxic and reliable solvent, instead of chemical solvents (39). To prepare the aqueous extract, 4.5 g of powdered *H. arenarium* and *G. aparine* leaves were mixed with 100 mL of distilled 18.2 MΩ/cm water (4.5% w/v) and boiled for 5 min. To remove plant residues, the extracts were first centrifuged (NF 800R, Nuve, Istanbul, Turkey) at 4025 *g* and 25 °C for 20 min and then filtered through Whatman filter paper No. 1 and were kept at 4 °C for further tests.

Nanoparticle synthesis optimisation

The synthesis of G-AgNPs and H-AgNPs was optimised by trial and error, using different parameters such as pH (6–10), temperature (25–80 °C), $AgNO_3$ concentration (0.1–2 mmol/L), and reaction time (0–240 min). The optimum green synthesis parameters for G-AgNPs were pH 8, temperature 70 °C, $AgNO_3$ concentration 1 mmol/L, and reaction time 4 h. Interestingly, the optimum synthesis parameters for H-AgNPs were different: pH 9, temperature 60 °C, $AgNO_3$ concentration 1 mmol/L (as in G-AgNPs), and reaction time 3 h. G-AgNPs and H-AgNPs analysed in this study were synthesised under these optimal conditions for biological activity.

To synthesise H-AgNPs 1 mL of aqueous *H. arenarium* extract was added dropwise to 20 mL of $AgNO_3$ solution in the 1:20 ratio (v:v) at 60 °C to obtain a concentration of 1 mmol/L. The pH of the mixture was then adjusted to 9 with 1 mol/L NaOH using a pH-meter (HANNA instruments HI 2211 pH/ORP Meter). The mixture was stirred on a magnetic stirrer at 60 °C for 3 h. To synthesise G-AgNPs, 1 mL of aqueous *G. aparine* extract was added dropwise to 20 mL of $AgNO_3$ solution in the 1:20 ratio (v:v) at 70 °C to reach a concentration of 1 mmol/L, and the pH of the mixture was then adjusted to 8. The mixture was stirred on a magnetic stirrer at 70 °C for 4 h.

The reaction was followed with a UV-Vis spectrophotometer (UV-1700, Shimadzu, Kyoto, Japan). The produced particles were collected by centrifugation at 9056 *g* and 25 °C for 30 min (Nüve NF 800R), washed three times with ultrapure water to remove unreacted plant residues and silver nitrate, and then lyophilised. All lyophilised nanoparticles were stored at -80 °C until further analysis. NF-1, NF-2, and NF-3 nanoformulations (NF) were prepared by combining G-AgNPs and H-AgNPs as follows: 1000 μg/mL G-AgNP + 1000 μg/mL H-AgNP (NF-1), 500 μg/mL G-AgNP + 1500 μg/mL H-AgNP (NF-2), and 1500 μg/mL G-AgNP + 500 μg/mL H-AgNP (NF-3).

Nanoparticle characterisation

The formation of nanoparticles was first confirmed visually based on the change in the colour of the reaction solution from yellow to brown. Analytically it was confirmed from the intensity of surface plasmon band absorption of nanoparticle solutions measured in the wavelength range of 200–800 nm at 25±0.1 °C using a UV-Vis spectrophotometer (UV-1700, Shimadzu). All measurements were made at a 1:10 dilution of the samples. For the blank we used ultrapure water.

The average size (hydrodynamic diameter) and polydispersity index (PDI) of nanoparticles were measured with dynamic light scattering (DLS), and the zeta potential with electrophoretic light scattering (ELS) using a Zetasizer Nano ZS (Malvern Instruments, Worcestershire, UK) equipped with a 4.0 mV He–Ne laser (633 nm) (7). Measurements were carried out in triplicate, at 25±0.1 °C, using the 0.8872 cP viscosity and 1.330 refractive indexes for the solutions and dielectric constant of 79 f(ka) 1.50 (Smoluchowski value). The number of runs and run durations were chosen automatically. All samples were diluted to a 1:10 ratio with distilled water before measurement.

The functional groups involved in both plant powders (*G. aparine* and *H. arenarium*) and the synthesised AgNPs (G-AgNPs and H-AgNPs) were determined using a Fourier transform-infrared (FT-IR) spectrophotometer (Shimadzu) (8). The analysis was performed in universal attenuation total reflectance (ATR) mode at 25±0.1 °C with a scanning spectrum of 800–3500 cm^{-1} wavenumber with 32 scans per sample and resolution of 4 cm^{-1}.

The surface morphology, topography, size, and size distribution of AgNPs were determined with both atomic force microscopy (AFM) (Shimadzu SPM 9600) and scanning electron microscopy (SEM) (FEI QUANTA 450 FEG, Thermo Fisher Scientific,

Waltham, MA, USA). AFM images were taken with the force constant of 0.02–0.77 N/m, tip height 10–15 nm, and silicon lever in contact mode (40). Freeze-dried powdered nanoparticles were fixed on metallic studs with double-sided conductive tape, then coated with gold under vacuum and analysed with SEM (7).

Antimicrobial activity measurement

The antimicrobial activity of G-AgNPs and H-AgNPs alone and in nanoformulations (NF-1, NF-2, and NF-3) was tested against *E. coli* (ATCC 25922), *S. aureus* (ATCC 25923), *C. albicans* (ATCC 10231), and *A. flavus* (ATCC 204304) *in vitro* using the broth microdilution method, which is a quantitative method. The results were obtained by spectrophotometric measurements (OD_{600} nm) and the standard plate counting method, as described by the Clinical & Laboratory Standards Institute (CLSI) standard (41, 42).

We prepared stock solutions of AgNPs and nanoformulations at a concentration of 2 mg/mL and serial dilutions in the range of 1–0.03125 mg/mL. 100 µL of the prepared samples were added to six wells each of the 96-well microplate. Microorganism suspension (10^6 CFU/mL) was added to each well to adjust the final volume in the wells to 200 µL. Microplates containing bacteria were incubated at 37 °C and microplates containing fungi at 28 °C for 16–18 h. After incubation, we determined minimum inhibition concentrations (MIC) and minimum bactericidal or fungicidal concentrations (MBC or MFC, respectively) by spectrophotometry (OD_{600} nm) and standard plate counting.

Statistical analysis

For statistical analysis we used the SPPS software version 22 (SPPS Inc., Chicago, IL, USA). All data are expressed as means ± standard deviations (SD) of three independent measurements. Statistical differences in MIC and colony counts between control and treated groups were analysed with the two-way analysis of variance (ANOVA) and significance set to $p<0.05$.

RESULTS

Nanoparticle properties

Figure 1 shows colour changes in the solution colour, which is attributed to the localised surface plasmon resonance (SPR) of metal nanoparticles (43–46). UV-Vis spectroscopy confirmed the formation of AgNPs with the characteristic SPR peak at 418 nm and 406 nm wavelengths for G-AgNPs and H-AgNPs, respectively.

Figure 2 shows that the particles were nanosized and highly monodisperse. Table 1 shows the average particle size, zeta potential, and PDIs of H-AgNPs and G-AgNPs. Because of excessive negative or positive zeta potential values (±30 mV), the electrostatic force between the nanoparticles prevents agglomeration of the NPs (47). These negative zeta potential values may be due to the presence of the stabilising agents (bioorganic components in the extract) acting as silver-reducing agents. Figure 3 shows the range of potentials for both H-AgNPs and G-AgNPs.

Figures 4a and 4c show the FT-IR spectra of *G. aparine* and *H. arenarium* plant powders, respectively. The vibrational stretches in the FT-IR spectrum of *G. aparine* at 3450, 2921–2848, 1378, and 1010 cm^{-1} correspond to the O–H stretch of an aromatic alcohol, aliphatic C-H stretch, the C=C stretch in the aromatic ring, and the alcohol C–O stretch, respectively. Despite lower peak intensities, the FT-IR spectrum of G-AgNPs is relatively similar to that of *G. aparine* (Figure 4b). Phytochemicals in *G. aparine* are responsible for the formation and stabilisation of G-AgNPs but also coat the surface of the nanoparticles (48).

The band at 1650 cm^{-1} in the spectrum of *H. arenarium* (Figure 4c) suggests that it may belong to the carbonyl stretch in the amide bond of the proteins, while the band at 1557 cm^{-1} may belong to the stretching vibrations of conjugated double bonds, indicating the presence of terpenoids or other aromatic plant components. The broad bands between 1100–1000 cm^{-1} may have formed due to ether interactions, suggesting the presence of flavanones in *H. arenarium*. The FT-IR spectrum of H-AgNPs (Figure 4d) shows that most of the functional groups in *H. arenarium* either disappeared or the existing peaks had large shifts in their positions. Compared to the FT-IR spectrum of *H. arenarium*, it suggests that the reduction, capping, and stabilisation of AgNPs are owed to the aromatic carbonyl, amide, and ether components as well as flavanone, protein, and terpenoid components, as reported elsewhere (22, 49).

Nanoparticle morphology

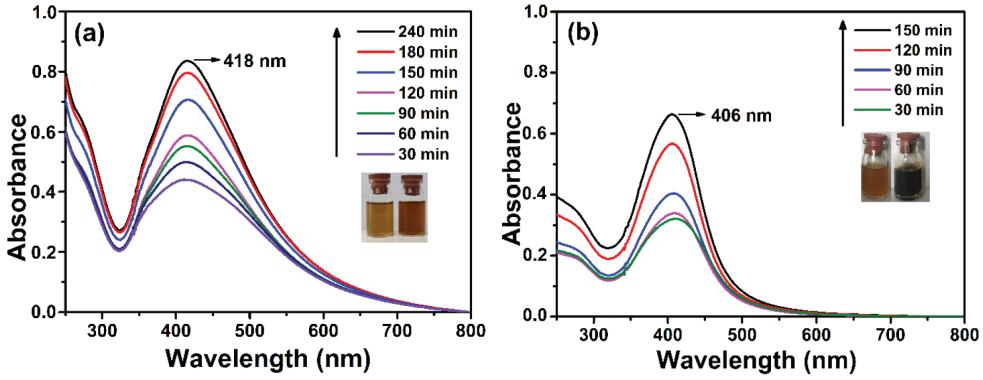

Figure 1 UV–Vis absorption spectra of a) G-AgNPs and b) H-AgNPs with different incubation times (0–240 min)

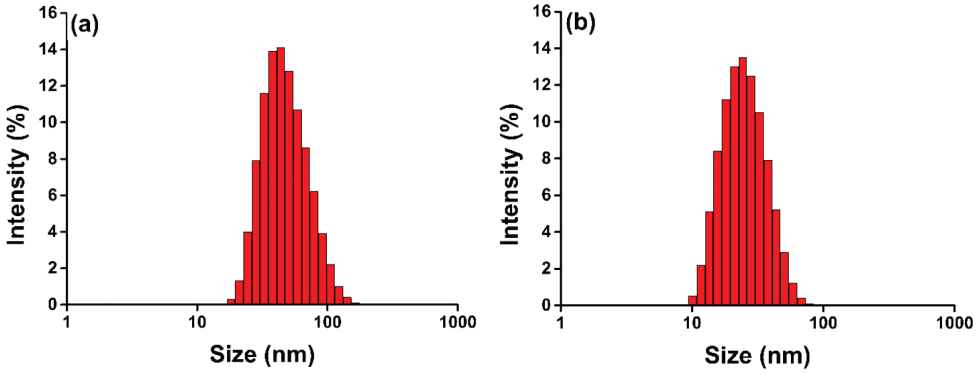

Figure 2 Particle size distribution of a) G-AgNPs and b) H-AgNPs

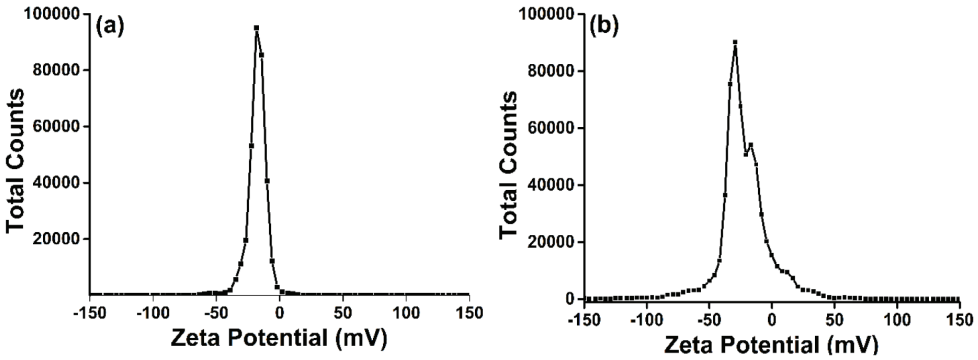

Figure 3 Zeta potential of a) G-AgNPs and b) H-AgNPs

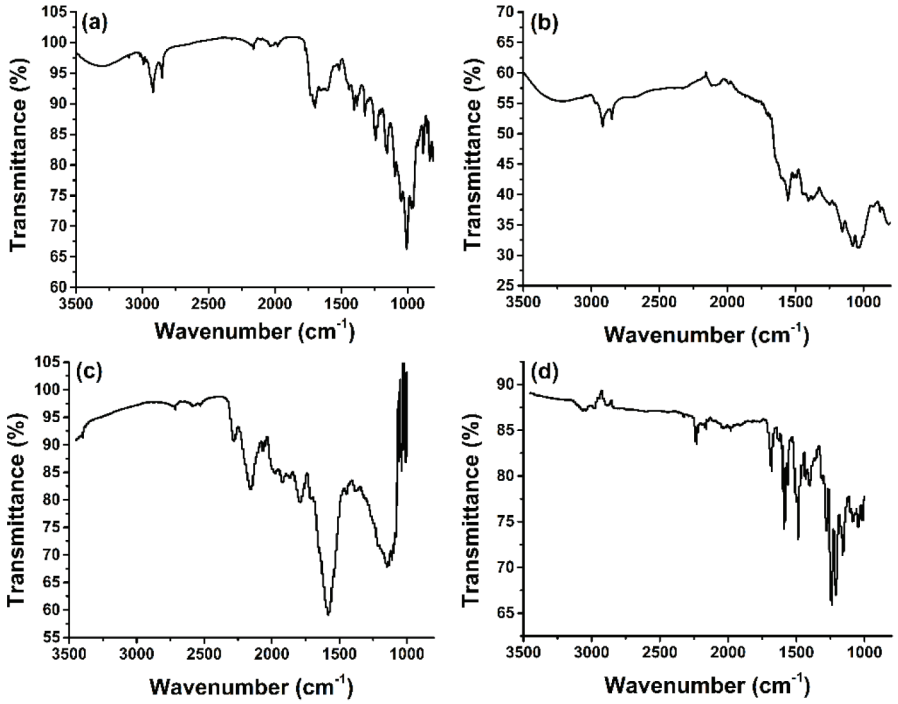

Figure 4 FT-IR spectrum of a) *G. aparine,* b) G-AgNPs, c) *H. arenarium*, and d) H-AgNPs

Table 1 Physicochemical properties of H-AgNPs and G-AgNPs

NPs	Particle Size (nm)	Zeta Potential (mV)	Polydispersity Index
H-AgNP	23.9±1.0	-21.3±2.7	0.285±0.034
G-AgNP	52.0±10.9	-17.9±0.9	0.280±0.032

Figures 5 and 6 show that most of the synthesised AgNPs have spherical and monodisperse distribution. The sizes of G-AgNPs are between 40 and 60 nm (Figures 5a and 6a), and the sizes of H-AgNPs are between 20 and 30 nm (Figures 5b and 6b). These values correlate with DLS findings.

Antimicrobial activity of nanoparticles and nanoformulations

Table 2 shows the minimum inhibitory, bactericidal, and fungicidal concentrations of G-AgNPs, H-AgNPs, and their three combinations against *E. coli, S. aureus, C. albicans,* and *A. flavus*. G-AgNPs were effective against *E. coli* and *C. albicans*, and H-AgNPs against *S. aureus* and *A. flavus*, which is evident from the Petri dish images (Table 3).

In turn, all nanoformulations combining H-AgNPs and G-AgNPs were significantly more effective against *E. coli* than their components alone, with the MIC lowered to 31.25 μg/mL for all three formulations, which points to a synergistic effect. In addition, NF-2 and NF-3 nearly halved the MIC and MBC of H-AgNPs alone against *S. aureus*, which points to an additive effect. Neither G-AgNPs or H-AgNPs alone or in combination showed antifungal effect, and their bactericidal effects against *E. coli* did not improve when combined.

DISCUSSION

Cell uptake of nanoparticles depends on particle size and so does their antimicrobial activity, which increases with smaller nanoparticles, as reported by Manoslava et al. (50) and Agnihotri et al. (51). The antimicrobial activity of G-AgNPs and combined nanoformulations against *E. coli* is higher than against other microorganisms tested in the study, which can be explained by the presence of a fine peptidoglycan layer and porins possessed by Gram-negative bacteria and the action of Ag^+ ions released by AgNPs (52–55). The somewhat higher negative zeta potential of H-AgNPs can, in turn, explain the antimicrobial activity against Gram-positive *S. aureus* and *A. flavus* (56). Ours and previous studies all seem to suggest that knowing the amount of dissolved Ag^+ released from the surface of AgNPs may shed more light on their antibacterial activity or cytotoxicity and we believe that future studies should be determining the amount of released Ag^+.

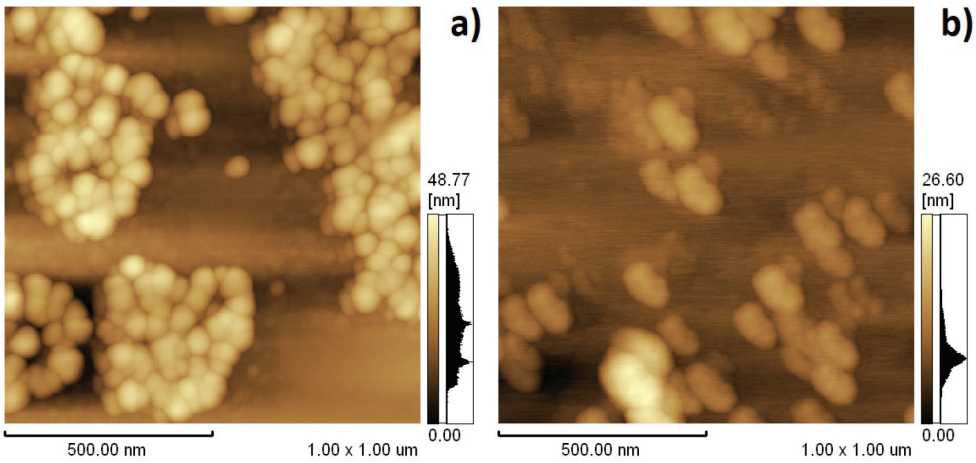

Figure 5 2-D Atomic force microscope images of a) G-AgNPs and b) H-AgNPs. Scan scale: 1×1 μm

Table 2 MBC/MFC and MIC values of samples according to the broth microdilution method

Test Sample	AgNP concentrations used in nanoformulations (μg/mL)	MIC (μg/mL) by microorganisms				MBC/MFC (μg/mL) by microorganisms			
		E. coli	*S. aureus*	*A. flavus*	*C. albicans*	*E. coli*	*S. aureus*	*A. flavus*	*C. albicans*
G-AgNPs		62.5	-	-	2000	125	-	-	-
H-AgNPs		-	125	500	-	-	-	-	-
NF-1	1000 G-AgNP + 1000 H-AgNP	31.25*	125	500	-	125	250	-	-
NF-2	500 G-AgNP + 1500 H-AgNP	31.25*	62.5	500	-	125	125	-	-
NF-3	1500 G-AgNP + 500 H-AgNP	31.25*	62.5	500	-	125	125	-	-

*$p<0.05$, NFs vs AgNPs. MBC – minimum bactericidal concentration; MFC – minimum fungicidal concentration; MIC – minimum inhibitory concentration

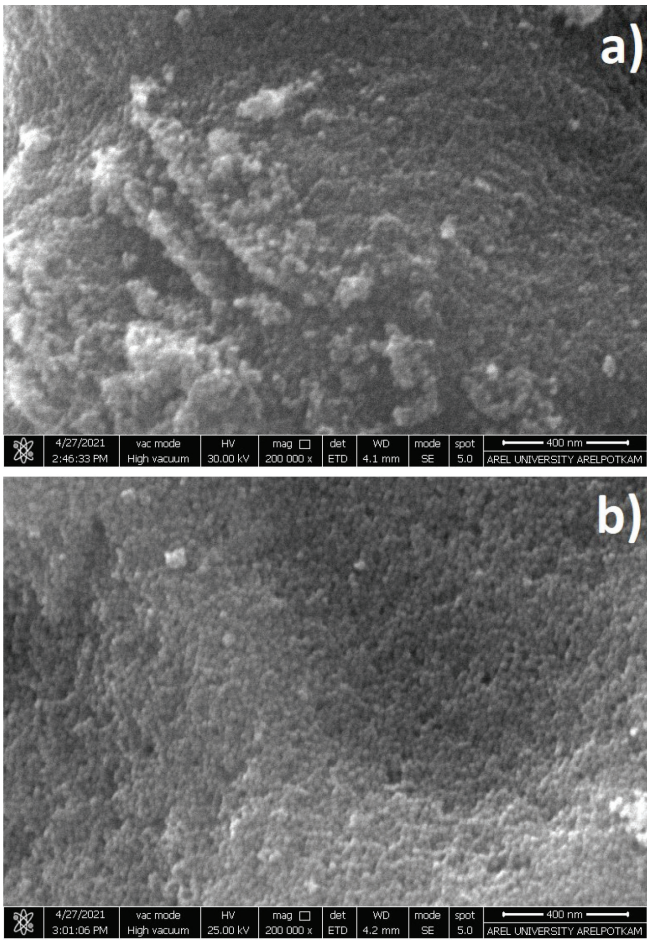

Figure 6 Scanning electron microscope images of a) G-AgNPs and b) H-AgNPs at 200,000× magnification

There are two interesting findings that we cannot yet explain. The first is that the combinations of G-AgNPs and H-AgNPs produced the same synergistic antimicrobial effect against *E. coli* regardless of their ratios. The second is that even though G-AgNPs showed inhibitory effect against *C. albicans* and H-AgNPs against *A. flavus*, none of their combinations inhibited *C. albicans*, yet maintained the inhibitory effect on *A. flavus*. We believe that further research should also try to explain this seeming paradox.

Despite these limitations of our study, our findings of the synergistic effects of the two synthesised nanoparticles when combined seem to support some earlier reports of improved antimicrobial effects by combinations of AgNPs with tomato, onion, acacia, neem, *Eucalyptus globulus, Trichophyton rubrum,* or garlic (57–61). One study that combined AgNPs synthesised with the rutin flavonoid and heliomycin antibiotic reported dose-dependent and synergistic antibacterial activity against *Aeromonas hydrophila* and *Pseudomonas fluorescens* (62).

In addition, we know that *H. arenarium* contains quercetin, chlorogenic acid, caffeic acid, and naringenin flavonoids, while *G. aparine* contains gallic acid, quercetin, tannic acid, and rutin (27, 28, 36). There are many studies showing the antimicrobial activity of these compounds alone (63–65). So, besides the combined effect of AgNPs with these plant components, the synergistic antimicrobial effect of the nanoformulations could be attributed to a synergy between plant components on the surface of AgNPs. This, however, calls for further investigation.

CONCLUSION

Our study is the first to report the antimicrobial activity of nanoformulations containing both G-AgNPs and H-AgNPs and the first to identify their synergism against *E. coli*. NF-2 and NF-3

Test Microorganism	Control	G-AgNP	H-AgNP	NF-1	NF-2	NF-3
E. coli*						
S. aureus						
A. flavus						
C. albicans						

Table 3 Petri dish images obtained by standard plate counting related to respective MICs. The dilution coefficient for *E. coli* is 10^2. There is no dilution for other microorganism. MIC – minimum inhibitory concentration

were more effective against *S. aureus* than G-AgNPs and H-AgNPs alone or combined in NF-1. This suggests that the antibacterial effect of H-AgNPs alone against *S. aureus* is further enhanced by what seems an additive effect of the NF-2 and NF-3 formulations. However, our study also raises a number of questions that need to be clarified by future studies, especially in terms of the mechanism of action involved.

Acknowledgments

This research was supported by the Scientific and Technological Research Council of Turkey (TUBITAK) under grant Nos. 1139B411900718 and 1139B411900634. For this research author Irem Coksu received a doctorate scholarship by the Republic of Turkey, Council of Higher Education.

REFERENCES

1. Alomar TS, AlMasoud N, Awad MA, El-Tohamy MF, Soliman DA. An eco-friendly plant-mediated synthesis of silver nanoparticles: Characterization, pharmaceutical and biomedical applications. Mater Chem Phys 2020;249:123007. doi: 10.1016/j.matchemphys.2020.123007
2. Gul AR, Shaheen F, Rafique R, Bal J, Waseem S, Park TJ. Grass-mediated biogenic synthesis of silver nanoparticles and their drug delivery evaluation: A biocompatible anti-cancer therapy. Chem Eng J 2021;407:127202. doi: 10.1016/j.cej.2020.127202
3. Hernández-Arteaga A, Nava JdJZ, Kolosovas-Machuca ES, Velázquez-Salazar JJ, Vinogradova E, José-Yacamán M, Navarro-Contreras HR. Diagnosis of breast cancer by analysis of sialic acid concentrations in human saliva by surface-enhanced Raman spectroscopy of silver nanoparticles. Nano Res 2017;10:3662–70. doi: 10.1007/s12274-017-1576-5
4. Küp FÖ, Çoşkunçay S, Duman F. Biosynthesis of silver nanoparticles using leaf extract of *Aesculus hippocastanum* (horse chestnut): Evaluation of their antibacterial, antioxidant and drug release system activities. Mater Sci Eng C Mater Biol Appl 2020;107:110207. doi: 10.1016/j.msec.2019.110207
5. Nejatzadeh F. Effect of silver nanoparticles on salt tolerance of *Satureja hortensis* l. during *in vitro* and *in vivo* germination tests. Heliyon 2021;7(2):e05981. doi: 10.1016/j.heliyon.2021.e05981
6. Roy A, Bulut O, Some S, Mandal AK, Yilmaz MD. Green synthesis of silver nanoparticles: biomolecule-nanoparticle organizations targeting antimicrobial activity. RSC Adv 2019;9:2673–702. doi: 10.1039/c8ra08982e
7. Derman S, Uzunoglu D, Acar T, Arasoglu T, Ucak S, Ozalp VC, Mansuroglu B. Antioxidant activity and hemocompatibility study of quercetin loaded Plga nanoparticles. Iranian J Pharm Res 2020;19:424–35. doi: 10.22037/ijpr.2020.1101000
8. Arasoglu T, Derman S, Mansuroglu B, Yelkenci G, Kocyigit B, Gumus B, Acar T, Kocacaliskan I. Synthesis, characterization and antibacterial activity of juglone encapsulated PLGA nanoparticles. J Appl Microbiol 2017;123:1407–19. doi: 10.1111/jam.13601
9. Folorunso A, Akintelu S, Oyebamiji AK, Ajayi S, Abiola B, Abdusalam I, Morakinyo A. Biosynthesis, characterization and antimicrobial activity of gold nanoparticles from leaf extracts of *Annona muricata*. J Nan Chem 2019;9:111–7. doi: 10.1007/s40097-019-0301-1
10. Ersoz M, Erdemir A, Duranoglu D, Uzunoglu D, Arasoglu T, Derman S, Mansuroglu B. Comparative evaluation of hesperetin loaded nanoparticles for anticancer activity against C6 glioma cancer cells. Artif Cells Nanomed Biotechnol 2019;47:319–29. doi: 10.1080/21691401.2018.1556213
11. Keshari AK, Srivastava R, Singh P, Yadav VB, Nath G. Antioxidant and antibacterial activity of silver nanoparticles synthesized by *Cestrum nocturnum*. J Ayurveda Integr Med 2020;11:37–44. doi: 10.1016/j.jaim.2017.11.003
12. Groneberg DA, Giersig M, Welte T, Pison U. Nanoparticle-based diagnosis and therapy. Curr Drug Targets 2006;7:643–8. doi: 10.2174/138945006777435245
13. Ahamed M, AlSalhi MS, Siddiqui M. Silver nanoparticle applications and human health. Clin Chim Acta 2010;411:1841–8. doi: 10.1016/j.cca.2010.08.016
14. Boca SC, Potara M, Gabudean A-M, Juhem A, Baldeck PL, Astilean S. Chitosan-coated triangular silver nanoparticles as a novel class of biocompatible, highly effective photothermal transducers for *in vitro* cancer cell therapy. Cancer Lett 2011;311:131–40. doi: 10.1016/j.canlet.2011.06.022
15. Ilyina T, Goryacha O, Toryanik E, Kulish I, Kovaleva A. Antimicrobial activity of the Genus *Galium* L. 2016;6:42–7. doi: 10.5530/pc.2016.1.8
16. Behravan M, Panahi AH, Naghizadeh A, Ziaee M, Mahdavi R, Mirzapour A. Facile green synthesis of silver nanoparticles using *Berberis vulgaris* leaf and root aqueous extract and its antibacterial activity. Int J Biol Macromol 2019;124:148–54. doi: 10.1016/j.ijbiomac.2018.11.101
17. Thakkar KN, Mhatre SS, Parikh RY. Biological synthesis of metallic nanoparticles. Nanomedicine 2010;6:257–62. doi: 10.1016/j.nano.2009.07.002
18. Ahmed S, Saifullah, Ahmad M, Swami BL, Ikram S. Green synthesis of silver nanoparticles using *Azadirachta indica* aqueous leaf extract. J Radiat Res Appl Sci 2016;9:1–7. doi: 10.1016/j.jrras.2015.06.006
19. Khalil MMH, Ismail EH, El-Baghdady KZ, Mohamed D. Green synthesis of silver nanoparticles using olive leaf extract and its antibacterial activity. Arab J Chem 2014;7:1131–9. doi: 10.1016/j.arabjc.2013.04.007
20. Xu J, Zhu X, Zhou X, Khusbu FY, Ma C. Recent advances in the bioanalytical and biomedical applications of DNA-templated silver nanoclusters. TrAC Trend Anal Chem 2020;124:115786. doi: 10.1016/j.trac.2019.115786
21. Castillo-Henríquez L, Alfaro-Aguilar K, Ugalde-Álvarez J, Vega-Fernández L, Montes de Oca-Vásquez G, Vega-Baudrit JR. Green synthesis of gold and silver nanoparticles from plant extracts and their possible applications as antimicrobial agents in the agricultural area. Nanomaterials 2020;10(9):1763. doi: 10.3390/nano10091763
22. Oves M, Rauf MA, Aslam M, Qari HA, Sonbol H, Ahmad I, Sarwar Zaman G, Saeed M. Green synthesis of silver nanoparticles by *Conocarpus Lancifolius* plant extract and their antimicrobial and anticancer activities. Saudi J Biol Sci 2022;29:460–71. doi: 10.1016/j.sjbs.2021.09.007
23. Loo YY, Chieng BW, Nishibuchi M, Radu S. Synthesis of silver nanoparticles by using tea leaf extract from *Camellia sinensis*. Int J Nanomedicine 2012;7:4263–7. doi: 10.2147/ijn.s33344
24. Yin IX, Zhang J, Zhao IS, Mei ML, Li Q, Chu CH. The antibacterial mechanism of silver nanoparticles and its application in dentistry. Int J Nanomedicine 2020;15:2555–62. doi: 10.2147/ijn.s246764

25. Ali ZA, Yahya R, Sekaran SD, Puteh R. Green synthesis of silver nanoparticles using apple extract and its antibacterial properties. Adv Mater Sci Engin 2016;2016:ID4102196. doi: 10.1155/2016/4102196
26. Senio S, Pereira C, Vaz J, Sokovic M, Barros L, Ferreira ICFR. Dehydration process influences the phenolic profile, antioxidant and antimicrobial properties of *Galium aparine* L. Ind Crop Prod 2018;120:97–103. doi: 10.1016/j.indcrop.2018.04.054
27. Bat Özmatara M. The effect of extraction Methods on Antioxidant and Enzyme Inhibitory Activities and Phytochemical Components of *Galium Aparine* L. Trakya Univ J Nat Sci 2021;22(1):e1–6. doi: 10.23902/trkjnat.772976
28. Vlase L, Mocan A, Hanganu D, Benedec D, Gheldiu A, Crisan G. Comparative study of polyphenolic content, antioxidant and antimicrobial activity of four *Galium* species (*Rubiaceae*). Digest J Nanomat Biostruct 2014;9(3):1085–94.
29. Atmaca H, Bozkurt E, Cittan M, Tepe HD. Effects of *Galium aparine* extract on the cell viability, cell cycle and cell death in breast cancer cell lines. J Ethnopharmacol 2016;186:305–10. doi: 10.1016/j.jep.2016.04.007
30. Shim J, Park M, Yang S. 574 Anti-inflammatory and antioxidant effects of *Galium Aparine* extract in macrophage RAW264.7 cells. J Invest Dermatol 2017;137(5 Suppl 1):S99. doi: 10.1016/j.jid.2017.02.596
31. Khan MA, Khan J, Ullah S, Malik SA, Shafi M. Hepatoprotective effects of *Berberis lycium*, *Galium aparine* and *Pistacia integerrima* in carbon tetrachloride (CCl4)-treated rats. J Postgrad Med Inst 2008;22(2):91–4.
32. Nejdet Ş, KALAYCI G. Chemical composition tannin and coumarin of *Helichrysum arenarium* [Altın otu bitkisinden (*Helichrysum arenarium*) tanen ve kumarinin kimyasal kompozisyonu, in Turkey]. Selçuk Üniversitesi Fen Fakültesi Fen Dergisi 2016;42(2):226–31.
33. Kurkina A, Ryzhov V, Avdeeva E. Assay of isosalipurposide in raw material and drugs from the dwarf everlast (*Helichrysum arenarium*). Pharm Chem J 2012;46:171–6. doi: 10.1007/s11094-012-0753-9
34. Grinev V, Shirokov A, Navolokin N, Polukonova N, Kurchatova M, Durnova N, Bucharskaya AB, Maslyakova GN. Polyphenolic compounds of a new biologically active extract from immortelle sandy flowers (*Helichrysum arenarium* (L.) Moench.). Russ J Bioorg Chem 2016;42:770–6. doi: 10.1134/S1068162016070086
35. Babotă M, Mocan A, Vlase L, Crisan O, Ielciu I, Gheldiu A-M, Vodnar DC, Crisan G, Păltinean R. Phytochemical analysis, antioxidant and antimicrobial activities of *Helichrysum arenarium* (L.) Moench. and *Antennaria dioica* (L.) Gaertn. flowers. Molecules 2018;23(2):409. doi: 10.3390/molecules23020409
36. Pljevljakušić D, Bigović D, Janković T, Jelačić S, Šavikin K. Sandy everlasting (*Helichrysum arenarium* (L.) Moench): Botanical, chemical and biological properties. Front Plant Sci 2018;9:1123. doi: 10.3389/fpls.2018.01123
37. Stanojević D, Ćomić L, Stefanović O, Solujić-Sukdoloak S. *In vitro* synergistic antibacterial activity of *Helichrysum arenarium*, *Inula helenium*, *Cichorium intybus* and some preservatives. Ital J Food Sci 2010;22(2):210–6.
38. Mohammad Azmin SNH, Abdul Manan Z, Wan Alwi SR, Chua LS, Mustaffa AA, Yunus NA. Herbal processing and extraction technologies. Sep Purif Rev 2016;45:305–20. doi: 10.1080/15422119.2016.1145395
39. Radovanović K, Gavarić N, Švarc-Gajić J, Brezo-Borjan T, Zlatković B, Lončar B, Aćimović M. Subcritical water extraction as an effective technique for the isolation of phenolic compounds of *Achillea* species. Processes 2023;11(1):86. doi: 10.3390/pr11010086
40. Silambarasan S, Abraham J. Biosynthesis of silver nanoparticles using the bacteria *Bacillus cereus* and their antimicrobial property. Int J Pharm Pharm Sci 2012;4(Suppl 1):536–40.
41. Wikler MA. Methods for dilution antimicrobial susceptibility tests for bacteria that grow aerobically: approved standard. CLSI (NCCLS) 2006;26:M7-A.
42. Duranoğlu D, Uzunoglu D, Mansuroglu B, Arasoglu T, Derman S. Synthesis of hesperetin-loaded PLGA nanoparticles by two different experimental design methods and biological evaluation of optimized nanoparticles. Nanotechnology 2018;29(39):395603. doi: 10.1088/1361-6528/aad111
43. Alsammarraie FK, Wang W, Zhou P, Mustapha A, Lin M. Green synthesis of silver nanoparticles using turmeric extracts and investigation of their antibacterial activities. Colloids Surf B Biointerfaces 2018;171:398–405. doi: 10.1016/j.colsurfb.2018.07.059
44. Hamedi S, Shojaosadati SA. Rapid and green synthesis of silver nanoparticles using *Diospyros lotus* extract: Evaluation of their biological and catalytic activities. Polyhedron 2019;171:172–80. doi: 10.1016/j.poly.2019.07.010
45. Parveen M, Kumar A, Khan MS, Rahman R, Furkan M, Khan RH, Nami SAA. Comparative study of biogenically synthesized silver and gold nanoparticles of *Acacia auriculiformi*s leaves and their efficacy against Alzheimer's and Parkinson's disease. Int J Biol Macromol 2022;203:292–301. doi: 10.1016/j.ijbiomac.2022.01.116
46. Dakshayani S, Marulasiddeshwara M, Kumar S, Golla R, Devaraja S, Hosamani R. Antimicrobial, anticoagulant and antiplatelet activities of green synthesized silver nanoparticles using Selaginella (Sanjeevini) plant extract. Int J Biol Macromol 2019;131:787–97. doi: 10.1016/j.ijbiomac.2019.01.222
47. Clogston JD, Patri AK. Zeta potential measurement. Methods Mol Biol 2011;697:63–70. doi: 10.1007/978-1-60327-198-1_6
48. Sreelekha E, George B, Shyam A, Sajina N, Mathew B. A comparative study on the synthesis, characterization, and antioxidant activity of green and chemically synthesized silver nanoparticles. BioNanoScience 2021;11:489–96. doi: 10.1007/s12668-021-00824-7
49. Sherin L, Sohail A, Mustafa M, Jabeen R, Ul-Hamid A. Facile green synthesis of silver nanoparticles using *Terminalia bellerica* kernel extract for catalytic reduction of anthropogenic water pollutants. Colloid Interface Sci Commun 2020;37:100276. doi: 10.1016/j.colcom.2020.100276
50. Manosalva N, Tortella G, Diez MC, Schalchli H, Seabra AB, Durán N, Rubilar O. Green synthesis of silver nanoparticles: effect of synthesis reaction parameters on antimicrobial activity. World J Microbiol Biotechnol 2019;35(6):88. doi: 10.1007/s11274-019-2664-3
51. Agnihotri S, Mukherji S, Mukherji S. Size-controlled silver nanoparticles synthesized over the range 5–100 nm using the same protocol and their antibacterial efficacy. RSC Adv 2014;4:3974–83. doi: 10.1039/c3ra44507k
52. Vishwasrao C, Momin B, Ananthanarayan L. Green synthesis of silver nanoparticles using sapota fruit waste and evaluation of their antimicrobial activity. Waste Biomass Valori 2019;10:2353–63. doi: 10.1007/s12649-018-0230-0
53. González-Fuenzalida RA, Moliner-Martínez Y, González-Béjar M, Molins-Legua C, Verdú-Andres J, Pérez-Prieto J, Campins-Falcó P. In situ colorimetric quantification of silver cations in the presence of silver nanoparticles. Anal Chem 2013;85:10013–6. doi: 10.1021/ac402822d

54. Lok C-N, Ho C-M, Chen R, He Q-Y, Yu W-Y, Sun H, Tam PK, Chiu JF, Che CM. Silver nanoparticles: partial oxidation and antibacterial activities. J Biol Inorg Chem 2007;12:527–34. doi: 10.1007/s00775-007-0208-z
55. Abbaszadegan A, Ghahramani Y, Gholami A, Hemmateenejad B, Dorostkar S, Nabavizadeh M, Sharghi H. The effect of charge at the surface of silver nanoparticles on antimicrobial activity against gram-positive and gram-negative bacteria: a preliminary study. J Nanomat 2015;2015:ID720654. doi: 10.1155/2015/720654
56. Rasmussen MK, Pedersen JN, Marie R. Size and surface charge characterization of nanoparticles with a salt gradient. Nat Commun 2020;11(1):2337. doi: 10.1038/s41467-020-15889-3
57. Kalwar K, Hu L, Li DL, Shan D. AgNPs incorporated on deacetylated electrospun cellulose nanofibers and their effect on the antimicrobial activity. Polym Adv Technol 2018;29:394–400. doi: 10.1002/pat.4127
58. Chand K, Cao D, Fouad DE, Shah AH, Dayo AQ, Zhu K, Lakhan MN, Mehdi G, Dong S. Green synthesis, characterization and photocatalytic application of silver nanoparticles synthesized by various plant extracts. Arab J Chem 2020;13:8248–61. doi: 10.1016/j.arabjc.2020.01.009
59. Chand K, Abro MI, Aftab U, Shah AH, Lakhan MN, Cao D, Mehdi G, Mohamed AMA. Green synthesis characterization and antimicrobial activity against *Staphylococcus aureus* of silver nanoparticles using extracts of neem, onion and tomato. RSC Adv 2019;9:17002–15. doi: 10.1039/c9ra01407a
60. Jafari Sales A, Shariat A. Synergistic effects of silver nanoparticles with ethanolic extract of *Eucalyptus globules* on standard pathogenic bacteria *in vitro*. Tabari Biomed Stu Res J 2020;2:13–21. doi: 10.18502/tbsrj.v2i3.4528
61. Robles-Martínez M, González JFC, Pérez-Vázquez FJ, Montejano-Carrizales JM, Pérez E, Patiño-Herrera R. Antimycotic activity potentiation of *Allium sativum* extract and silver nanoparticles against *Trichophyton rubrum*. Chem Biodivers 2019;16(4):e1800525. doi: 10.1002/cbdv.201800525
62. Essawy E, Abdelfattah MS, El-Matbouli M, Saleh M. Synergistic effect of biosynthesized silver nanoparticles and natural phenolic compounds against drug-resistant fish pathogens and their cytotoxicity: An *in vitro* study. Mar Drugs 2021;19(1):22. doi: 10.3390/md19010022
63. Nguyen TLA, Bhattacharya D. Antimicrobial activity of quercetin: an approach to its mechanistic principle. Molecules 2022;27(8):2494. doi: 10.3390/molecules27082494
64. Stojković D, Petrović J, Soković M, Glamočlija J, Kukić-Marković J, Petrović S. *In situ* antioxidant and antimicrobial activities of naturally occurring caffeic acid, p-coumaric acid and rutin, using food systems. J Sci Food Agric 2013;93:3205–8. doi: 10.1002/jsfa.6156
65. Li G, Wang X, Xu Y, Zhang B, Xia X. Antimicrobial effect and mode of action of chlorogenic acid on *Staphylococcus aureus*. Eur Food Res Technol 2014;238:589–96. doi: 10.1007/s00217-013-2140-5

Nova strategija za postizanje visoke antimikrobne djelotvornosti: zelena sinteza formulacija srebrnih nanočestica pomoću biljnih vrsta *Galium aparine* **i** *Helichrysum arenarium*

Srebrne se nanočestice (AgNP), koje su već neko vrijeme u središtu pažnje zbog svojih antimikrobnih svojstava, mogu proizvoditi i zelenom sintezom. Cilj je ovog istraživanja bio (i) opisati (karakterizirati) zelenu sintezu različitih AgNP-a pomoću vodenih ekstrakata čekinjaste broćike (*Galium aparine*) (G-AgNPs) i pješčarskoga smilja (*Helichrysum arenarium*) (H-AgNPs), dobivenih metodom mikrovalne ekstrakcije, te (ii) utvrditi antimikrobno djelovanje kombinacije tih dvaju nanosustava u različitim omjerima. Oblikovanje nanočestica i kemijske reakcije utvrđene su pomoću UV-Vis spektroskopije. Veličina G-AgNP-a bila je 52,0±10,9 nm, njihov polidisperzivni indeks (PDI) 0,285±0,034, a zeta potencijal -17,9±0,9 mV. Osobine H-AgNP-a bile su sljedeće: veličina 23,9±1,0 nm, PDI 0,280±0,032, a zeta potencijal -21,3±2,7 mV. Mikroskopijom atomskih sila (engl. *atomic force microscopy*, krat. AFM) i pretražnom elektronskom mikroskopijom (engl. *scanning electron microscopy*, krat. SEM) potvrđeno je da su čestice monodisperzivne i sferične. Rezultati infracrvene spektroskopije s Fourierovom transformacijom (engl. *Fourier transform-infrared spectroscopy,* krat. FT-IR) potvrdili su prisutnost reduktivnih agenasa koji su stabilizirali srebrne nanočestice. Zatim su pripremljene tri formulacije nanočestica (NF-1, NF-2 i NF-3) kombinacijom sintetiziranih nanočestica u različitim omjerima, a njihova antimikrobna djelotvornost testirana je na mikroorganizmima *E. coli, S. aureus, C. albicans* i *A. flavus*. Naše je istraživanje prvo koje dokazuje da kombinacija srebrnih nanočestica dobivenih iz dvaju bioloških izvora može biti djelotvorna te da ima poboljšano antibakterijsko djelovanje protiv *E. coli* i *S. aureus* u odnosu na zasebne nanosustave. Minimalna inhibicijska koncentracija kombinacija iznosila je 31,25 μg/mL za *E. coli* u svim nanoformulacijama te 62,5 μg/mL za *S. aureus* s NF-1, odnosno 125 μg/mL s NF-2 i NF-3, a minimalne inhibicijske koncentracije G-AgNP-a odnosno H-AgNP-a zasebno su iznosile 62,5 μg/mL za *E. coli* (G-AgNP), odnosno 125 μg/mL za *S. aureus* (H-AgNP). To kombinirano antibakterijsko djelovanje protiv *E. coli* bilo je sinergijsko, a protiv *S. aureus* naizgled aditivno. S obzirom na ovako obećavajuće rezultate, smatramo da naše istraživanje daje smjer za razvoj novih strategija u antibakterijskom liječenju.

KLJUČNE RIJEČI: *A. flavus*; antimikrobni nanosustavi; biljkni ekstrakti; *C. albicans*; *E. coli*; *S. aureus*; sinergijsko djelovanje